

TiO₂-assisted photocatalytic degradation of diclofenac, metoprolol, estrone and chloramphenicol as endocrine disruptors in water

Bożena Czech · Katarzyna Rubinowska

Received: 31 October 2012 / Accepted: 22 January 2013 / Published online: 7 February 2013
© The Author(s) 2013. This article is published with open access at Springerlink.com

Abstract The photocatalytic oxidation of diclofenac, metoprolol, estrone and chloramphenicol was tested in the tube reactor using different commercially available TiO₂. The photocatalysts were characterized using BET, XRD and SEM. The studied photocatalysts differed in S_{BET}, pore volume and rutile presence. It was observed that generally anatase TiO₂ possessed the highest activity in the photocatalytic oxidation of diclofenac, chloramphenicol and estrone. The presence of rutile enhanced the photooxidation of metoprolol. In case of the other pollutants, however, rutile diminished the photooxidation efficiency. The most effective in the reduction of the COD parameter of treated water was anatase with 21 nm crystals. The photooxidation of all studied pollutants can be described by the pseudo-first order kinetics with the values ranging from $0.46 \times 10^{-2} \text{ min}^{-1}$ in case of estrone removal over Tytanpol (Z.A. Police, Poland) to $1.87 \times 10^{-2} \text{ min}^{-1}$ for the removal of chloramphenicol over TiO₂ 21 nm (Sigma-Aldrich). The highest initial reaction rates were obtained for metoprolol removal over TiO₂ 21 nm (Sigma-Aldrich) $1.9 \times 10^{-6} \text{ mol dm}^3 \text{ min}^{-1}$ being three times higher than that determined for estrone photocatalytic oxidation over TiO₂ (Sigma-Aldrich).

Keywords Photocatalysis · TiO₂ · PPCPs · AOPs · EDCs

B. Czech (✉)
Department of Environmental Chemistry, Faculty of Chemistry,
Maria Curie-Skłodowska University, Pl. M. Curie-Skłodowskiej 5,
20-031 Lublin, Poland
e-mail: bczech@hektor.umcs.lublin.pl

K. Rubinowska
Department of Plant Physiology, University of Life Sciences
in Lublin, Akademicka 13, 20-950 Lublin, Poland

1 Introduction

In the recent years there is observed a great progress in the field of photocatalytic studies (Friedmann et al. 2010; Herrmann 2010) and the application of Advanced Oxidation Processes (AOPs) in the remediation of contaminated air, water and soil. Beside AOPs, heterogeneous photocatalysis has gained the attention as promising technique that can be used as alternatives or as a complement to conventional wastewater treatment (polishing step). It enables the mineralization of completely recalcitrant contaminants (including organics, inorganics, metals and pathogens) into CO₂, H₂O and small amount of simple inorganic compounds. The photocatalysis is described as the generation of *OH radicals. The main advantage of this system is that radicals can be generated chemically, photochemically, and photocatalytically, depending on the treatment condition and requirements.

TiO₂ is the mostly studied photocatalyst. The application of suspended TiO₂, beside its unquestionable advantages such as biological and chemical resistance, safety, low price and affordability, is connected however with expensive recycling and recovery of the photocatalyst (Dolat et al. 2012).

One of the factors affecting the photocatalytic oxidation over TiO₂ is the initial adsorption of the contaminants on the TiO₂ surface. Solution can be supported TiO₂ photocatalysts prepared using different adsorptive materials (Herrmann 2010). Many affords have been taken to enhance the adsorption and different types of supports for TiO₂ have been tested including silica, perlite, activated carbon (Yao et al. 2010), glass (Fernandez et al. 1995), clay, zeolites and many others. The supported porous catalysts with higher surface area are often being chosen, since, apart from easier disposal, they ensure a high density of active centers for reactions and an enhanced light harvesting because of light reflection and scattering by the pores (Friedmann et al. 2010).

The successful application of TiO₂ in the removal of different organic pollutants such as dyes (Yao et al. 2010) or phenols (Emeline et al. 2012) has encouraged the studies dealing with the removal of recently recognized wastewater pollutants—Pharmaceuticals and Personal Care Products (PPCPs). PPCPs in the environment are derived from usage by individuals and pets (in the households and intensive animal breeding farms as growth enhancers), disposal of outdated medications in sewage systems, release of treated and untreated hospital and veterinary wastes to domestic sewage systems, transfer of sewage solids (biosolids) to land, industrial waste streams and releases from aquaculture of medicated feeds, etc. (Ellis 2006; Fatta-Kassinos et al. 2011; Qin et al. 2012). A total of 170 pharmaceutical chemicals are estimated to be used in excess of 1 tone per year (Ellis 2006). Many of PPCPs are not new chemicals and have been present in wastewater for many decades but only now they are being recognized as potentially significant water pollutants.

Depending on their properties, PPCPs can enter the aquatic environment or remain adsorbed on solid particles through electrostatic forces. Many PPCPs are highly bioactive, most are polar, optically active, and all are present in the environment at extremely low concentrations ranging from ng dm⁻³ to μg dm⁻³ (e.g. in natural waters, wastewater, sediments and sludge) (Ellis 2006).

Conventional treatment methods are not able to degrade them completely because they are persistent against biological degradation and natural attenuation. It has resulted in their frequent presence in the wastewater. In 2004 there was identified 2986 PPCPs in treated wastewater (Sanderson et al. 2004). PPCPs introduced into the aquatic environment are considered to be that ensures a vacuum of as Endocrine Disrupting Compounds, EDCs that mimic, inhabit or enhance the action of hormones (Gultekin and Ince 2007).

UV irradiation (Lopez et al. 2003; Kasprzyk-Hordern et al. 2009; Kim et al. 2009; Jelic et al. 2010; Fatta-Kassinos et al. 2011) and ozonation (Ternes et al. 2003; Álvarez et al. 2011), were successfully used to remove different PPCPs. β-blockers (metoprolol, propranolol, atenolol) (Álvarez et al. 2011; Ioannou et al. 2011; Hapeshi et al. 2010), antibiotics (ofloxacin, amoxicillin) (Hapeshi et al. 2010), psychiatric drugs (carbamazepine) (Kim et al. 2009), and analgesics and anti-inflammatory drugs (diclofenac) (Kim et al. 2009; Achilleos et al. 2010) were removed from water and wastewater using TiO₂-assisted photocatalysis.

There is interesting to study the photocatalytic removal of some typed representatives of PPCPs from water using commercially available TiO₂ anchored to reactor walls. The main aim of the studies though was the determination of the catalytic activity of wall-deposited TiO₂ photocatalysts in the removal of PPCPs belonging to different therapeutic class of pharmaceuticals.

2 Experimental

2.1 Chemicals

As the photocatalyst were used 4 commercially available TiO₂ photocatalyst: TiO₂—Tytanpol, Police Z.A. Poland (catalyst T1), and TiO₂—Sigma-Aldrich (T2), Hombikat—Sigma-Aldrich (T3) and TiO₂-S21 Sigma-Aldrich (T4). As the substrates analgesics and anti-inflammatory drug: diclofenac sodium salt (DFC), antibiotic: chloramphenicol (CPL), β-blocker: metoprolol titrate salt (Mt), natural estrogen: estrone (E1) were supplied from Sigma-Aldrich. Ethanol was used as co-solvent for E1 in aqueous solution.

2.2 Photocatalysts preparation

14.6 g of proper TiO₂ was mixed with aluminum cement (142 g) and 40 cm³ of liquid glass and 40 cm³ (or 80 cm³ in case T3) of water. The 25 cm long tube with the internal diameter 48 mm was fulfilled with the mixture for 10 min to make the uniform layer on the aluminum tube. The excess of the mixture that did not adsorbed after 10 min was thought out. Prepared tubes were dried for 24 h at room temperature before use.

2.3 Photocatalysts characterization

The specific surface area of the catalysts was determined on the basis of low-temperature nitrogen adsorption–desorption method in a volumetric analyzer AUTOSORB-1CMS, Quantachrome Instruments, (USA) that ensures a vacuum of at least 2×10^{-6} kPa. Standard Brunauer-Emmett-Teller (BET) method for nitrogen adsorption data was used to calculate S_{BET} of the photocatalysts. Consequently, the total pore volume (V_p) of mesopores was estimated from a single point adsorption at a relative pressure of 0.985 and the pore size distribution was obtained from desorption branch of the isotherm according the Barrett-Joyner-Halenda (BJH) procedure.

SEM studies were conducted on a Tesla BS-301 microscope Quanta 3D FEG operating at 15.0 keV. X-ray diffraction (XRD) on Diffractometer HZG-4 (Carl Zeiss Jena) using monochromatic Cu Kα radiation was used to determine the phase composition of the catalysts and estimation of the crystal size of TiO₂. The X-ray patterns were scanned in 2θ range of 20°–80° with a step 0.05°.

The quantitative property of treated wastewater was determined using COD and UV–Vis spectroscopic measurements. COD/COD_0 and c/c_0 have been used to calculate the conversion, where c_0 or COD_0 was the initial concentration or initial COD of a pollutant, respectively and c or COD was the concentration of the compounds or COD under study that did not react at a steady state.

2.4 Photocatalytic studies

The photocatalytic oxidation of 50 mg dm⁻³ DFC, CPL, E1 and Mt was conducted in the tube reactor, equipped with the UV lamp (254 nm, 0.7 kW) emitting 95 % UV, with the light intensity 2 mW cm⁻². Such concentrations were chosen to allow assessing the process efficiency within a measurable time scale, and determining the residual concentrations with the analytical techniques (UV–Vis spectroscopy, COD measurements) employed in this work.

The lamp was placed vertically inside the reaction vessel and housed in an inner glass tube (Fig. 1). The tube with photocatalyst was placed in the reactor in the central part and was connected at the top and at the bottom with two other tubes without photocatalyst. The reactor volume actively irradiated by UV was 0.3 dm³. The reactor was fulfilled at the volumetric flow of 4.45 cm³ min⁻¹ before the lamp was turned on for 24 h to maintain the equilibrium and in order to know the adsorption into the samples.

The UV–Vis absorption spectra were recorded in a wavelength range of 190–300 nm in a 10 mm quartz cell in Varian Cary 4000 Spectrophotometer, in the following conditions: scan rate 600 nm·min⁻¹; time response: 0.1 s; spectral band 2 nm. The concentration of studied pollutants was measured from the absorbance at the proper wavelength (Table 1; Fig. 2) by using a calibration curve. The COD was determined using bichromate method.

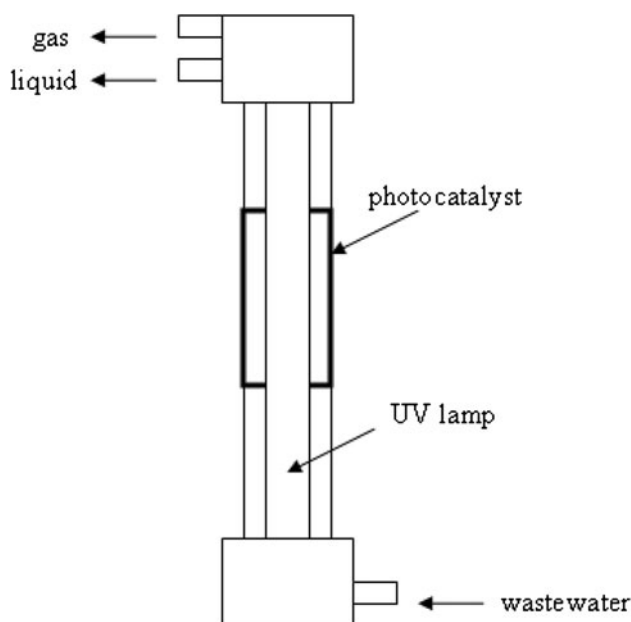


Fig. 1 Reactor scheme

3 Results and discussion

3.1 Characterizations of the samples

3.1.1 BET

The applied materials are mesoporous with the presence of mesopores with uniform pore size distribution centered at 10 nm (Table 2).

The BET surface area of T1 and T2 was ca. 12 m² g⁻¹ and T3 and T4 was 55–61 m² g⁻¹. The pore volume of the photocatalysts was 0.025 cm³ g⁻¹ for low surface area photocatalysts and 0.13–0.15 cm³ g⁻¹ for its counterparts with higher surface area. However, there was no hysteresis loop at relative pressures of 0.4–0.99 in the sample T1 and its BET surface area was 12 m² g⁻¹, further confirming the absence of mesopores in the T1.

3.1.2 SEM

The scanning microscopy was applied to study the surface morphology of the samples. The morphology of the samples presented in Fig. 3 looks similarly.

The photocatalysts are in the form of small agglomerates of crystals with the diameter of ca. 0.2–0.25 μm. The surface is full of voids and pores. The SEM micrographs were used to estimate the diameter of the primary structure of TiO₂ and obtained value 20 nm is in good agreement with XRD data.

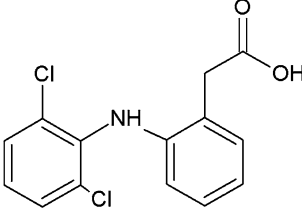
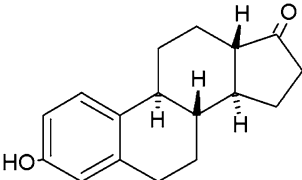
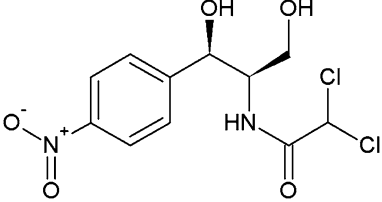
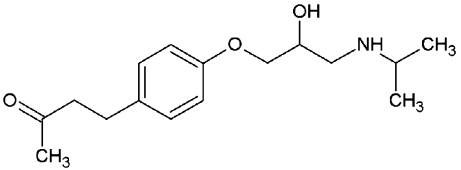
3.1.3 XRD

XRD was applied to determine the phase composition of studied photocatalysts. All XRD spectra presented in the Fig. 4 looks similarly and the peaks confirming anatase structure are directly observed. According to JCPD 21-1272, the peaks at 2Θ of about 25.2, 37.9, 48.3, 53.8, 62.7 and 68.9 (depicted in Fig. 4 as A) are representing the presence of anatase structure (planes 1 0 1, 1 0 3, 2 0 0, 1 0 5, 2 1 3 and 1 1 6, respectively). In the XRD spectra of T2 and T3 the presence of rutile crystallites was evidenced at 2Θ of 27.4 and 37.1 (JCPDS 21-1276) depicted in Fig. 5 as R. The crystalline sizes of samples (Table 2) were calculated applying Scherrer equation (Eq.1):

$$D = \frac{K \cdot \lambda}{\beta \cdot \cos \theta} \quad (1)$$

where D is the crystal size in nanometer, K is the factor of the crystal shape (0.94), λ is the wavelength of X-Ray radiation (0.1548 nm for Cu K α radiation), β is the full width at half-maximum and θ is the peak position.

Table 1 The properties of studied PPCPs

PPCPs	λ_{max} (nm)	Molecular weight (g mol ⁻¹)	pKa	log <i>K</i> _{ow}
 <p>Diclofenac</p> <p>2-(2-(2,6-dichlorophenylamino) phenyl) acetic acid CAS No. 15307-86-5</p>	276	318.13	4.51	0.7
 <p>estrone</p> <p>3-hydroxy-13-methyl-6,7,8,9,11,12,13,14,15,16-decahydrocyclopenta [a]phenanthren-17-one</p>	222	270.37	10.4	3.13
 <p>chloramphenicol</p> <p>2,2-dichloro-<i>N</i>-[1,3-dihydroxy-1-(4-nitrophenyl)propan-2-yl]acetamide</p>	275	323.132	9.5	2.055
 <p>metoprolol</p> <p>(<i>RS</i>)-1-(isopropylamino)-3-[4-(2-methoxyethyl)phenoxy]propan-2-ol</p>	222	267.36		β -blocker

Concluding the data obtained by XRD, SEM and BET TiO_2 : T2 and T3 possessed rutile phase and differed in S_{BET} and V_p . The anatase photocatalysts also varied in S_{BET} and V_p . T1 and T2 that beside the difference in rutile presence had the similar value of the other parameters. The same was observed for T2 and T4.

3.2 Photocatalytic test

3.2.1 DFC photoremoval

It can be observed (Fig. 5) that DFC was effectively removed from water using photocatalytic oxidation. The best changes

in the water quality were observed during first 20–40 min of treatment and resulted in at least 65 % decrease of the concentration of studied pollutant.

The highest DFC c/c_0 decrease was determined using T1 photocatalyst but generally all anatases revealed similar activity. The presence of rutile in TiO₂ slightly diminished the photocatalytic efficiency. COD of treated DFC water, however, revealed that mineralization of DFC over T3 preceded almost at the same level that photocatalytic oxidation during first 2 h of treatment. It may indicate that the mineralization was as fast as the DFC photoremoval. The general tendency of the removal of DFC and its photooxidation products over all studied photocatalysts was similar—the highest decrease was observed during first 40 min of treatment and the further photocatalytic oxidation did not result in the total elimination of studied pollutant. Taking into consideration the type of the photocatalysts the efficiency of DFC removal over the studied photocatalysts was decreasing in the following order: T1 > T4 > T2 > T3.

Some of end-products are expected to be quite recalcitrant to further decomposition. It may result from the presence of intermediates that absorb at studied range and, thus, misleadingly contribute to the organic content of the Dc curve. They may also adsorb onto the catalyst surface and, thus, do not contribute to the measured COD (He et al. 2011).

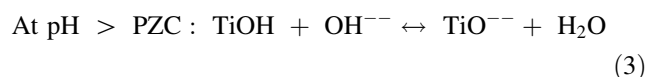
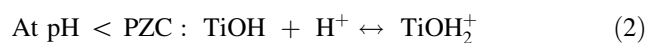
The tendency of DFC removal (described as COD decrease) over T2 was the deepest during 60–80 min and

then the COD reduction was maintained at the same level indicating that produced by- and end-products of DFC photooxidation were stable and resistant to further oxidation. Although the tendency of COD reduction using T1, T3 and T4 was similar, the photocatalysts differed in final effectiveness—the results obtained over T1 (with the smallest crystals) were almost two times better than over T3. The presence of rutile in comparison to anatase expectedly diminished the final results however; the small fraction of rutile significantly accelerated the DFC decomposition. T1 that is described by the producer as anatase contains however a small addition of rutile, (XRD peak at 27.4) revealed the highest photoactivity. The key is though the small amount of rutile, not pure anatase structure.

The studies of Zhang et al. 2011 indicated that the self-sensitized photooxidation of pollutants may be observed. $^{\bullet}\text{OH}$, $^1\text{O}_2$ and $\text{O}_2^{\bullet-}$ were involved in the DCF photooxidation. The photodegradation of DCF was then the sum of the degradation by direct photolysis and self-sensitization.

The primary transformation product of diclofenac under the studied conditions was (8-chloro-9H-carbazol-1-yl)acetic acid ($\lambda_{\text{max}} = 254 \text{ nm}$). That was in agreement with the results obtained by Zhang et al. (2011), Martínez et al. (2011) or Qin et al. (2012). (8-chloro-9H-carbazol-1-yl)acetic acid may be obtained as the result of $^{\bullet}\text{OH}$ addition to 2-(8-chloro-9H-carbazol-1-yl)acetic acid, the product of photocyclization to the monohalogenated carbazole, involving loss of chlorine and hydrogen atoms, followed by structural rearrangement resulting in the formation of a new ring.

The pH of DFC water was 7.34 and taking into consideration the pH_{pzc} of different TiO₂ that lies in the pH range of 4.5–7.0 (Chong et al. 2010), it can be observed that at pH > PZC(TiO₂), the catalyst surface is negatively charged and repulse the anionic compounds in water. In the studied region of pH the surface charge density distribution for these TiO₂ catalyst clusters TiOH is $\geq 80 \%$ at $3 < \text{pH} < 10$, according to the following water equilibrium equations (Eqs. (2) and (3)):



The solution pH affects the degree of dissociation of organic, the extent of adsorption in their ionized form and hence the observed reaction rates. Electrostatic favored adsorption results in sensitivity of TiO₂ to pH adjustments. Electroneutral adsorption cannot be neglected being the dominant manner of adsorption of organic acids in solution (Friedmann et al. 2010). A rapid and simultaneous chemisorption of dissociated H⁺ and the deprotonated organic acid in the very close vicinity of the surface takes

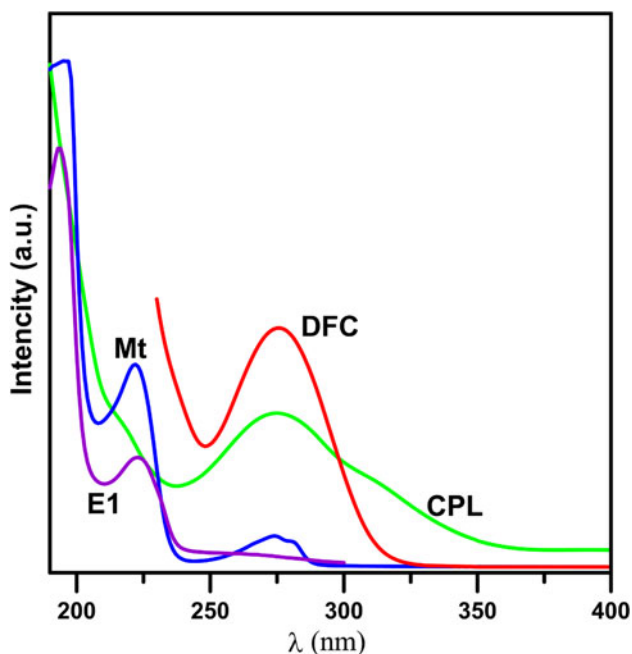


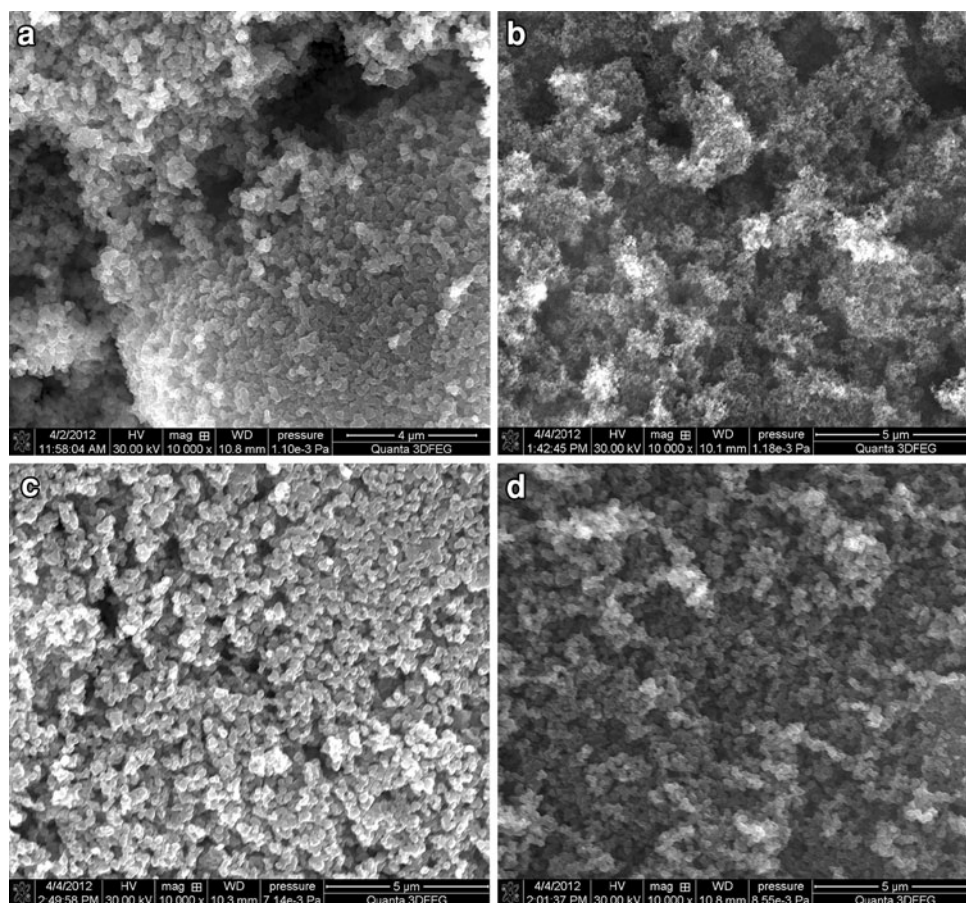
Fig. 2 UV-Vis spectra of studied pollutants (Kumar et al. 2010; Kasperek et al. 2011) (Color figure online)

Table 2 The physicochemical properties of the studied photocatalysts

Catalyst	BET surface ($\text{m}^2 \text{g}^{-1}$)	The pore volume ($\text{cm}^3 \text{g}^{-1}$)	Mean pore diameter (\AA)	The presence of rutile	Crystallinity (nm)*
T1	12.08	0.024620	81.53	-/+	19
T2	11.50	0.025734	89.50	+	59
T3	61.03	0.150906	98.90	+	20
T4	55.33	0.134603	97.30	-	21

* Calculated applying Scherrer equation and the peak

Fig. 3 SEM micrographs of the studied photocatalysts: **a** T1, **b** T2, **c** T3, **d** T4



place. The exposed facets either of rutile (110) or anatase (100) containing dangling Ti and O atoms closed to each other make titania an optimum surface for electroneutral adsorption. The pH of the solution after treatment finally increased to the value 8.

3.2.2 CPL photooxidation

The photocatalytic photooxidation of CPL as the representatives of antibiotics is presented in Fig 6.

It can be observed that the best results were again obtained during first 40–60 min of treatment. The further irradiation still did not result in the total removal of studied pollutant from water. The decrease of the CPL concentration

using anatase TiO_2 was similar. During the first 60 min the removal of CPL proceeded almost linearly and then there were observed a small decrease of CPL concentration. It indicates that the products of photooxidation of CPL (glycolic aldehyde, dichloroacetamide and 4-nitrobenzaldehyde) are resistant to further photooxidation.

The c/c_0 reduction was the most effective over all photocatalysts except T2. It can be observed that the photooxidation of CPL proceeded faster over the smaller crystals of TiO_2 . COD of treated water containing CPL was also significantly decreasing during first hour of treatment. In case of anatase containing TiO_2 there can be observed a change in the shape of the curve: after 45 min the COD reduction tendency changed from linear to logarithmic

dependency indicating that in the first minutes the COD reduction was connected with CPL removal and then the COD decrease was combined with by-products photooxidation. The photocatalysts with enhanced surface area were more effective than their low surface area counterparts.

The lowest COD reduction however was determined using T1 and T2 photocatalysts indicating that the key role in the removal of CPL and its oxidation products plays the surface area. pH of the solution was 6.888 and at pH below pH_{pzc} the surface of TiO₂ is positively charged and adsorption by electrostatic forces occurs. After the treatment the pH value 7 was maintained.

3.2.3 E1 photoremoval

The photocatalytic removal of E1 was observed over all studied photocatalysts (Fig 7).

The lowest activity in E1 removal from water was determined for T2 photocatalyst. There was more than 60 % of initial concentration of E1 left without decomposition. The highest decrease of the E1 concentration during treatment was observed over T4. In case of this pollutant it can be also noted that the similar general tendency for low and high surface area photocatalysts can be observed. Although E1 was photooxidized, its oxidation products were stable and resistant to further photooxidation. Again there can be observed the two steps oxidation over all photocatalysts. The key time of photocatalytic oxidation was first 45-60 min. The obtained results may indicate that the decomposition of E1 was fast but the products of the

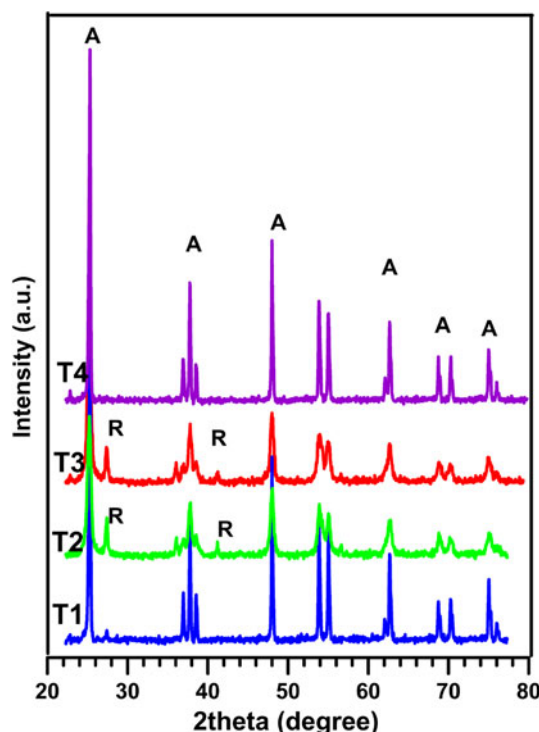


Fig. 4 XRD spectra of studied photocatalysts, A anatase, R rutile (Color figure online)

photooxidation (e.g. ketohydroperoxide) are more stable for the further photooxidation.

The pH of E1 water was 7.798 and taking into consideration the pH_{pzc} of studied materials adsorption of the

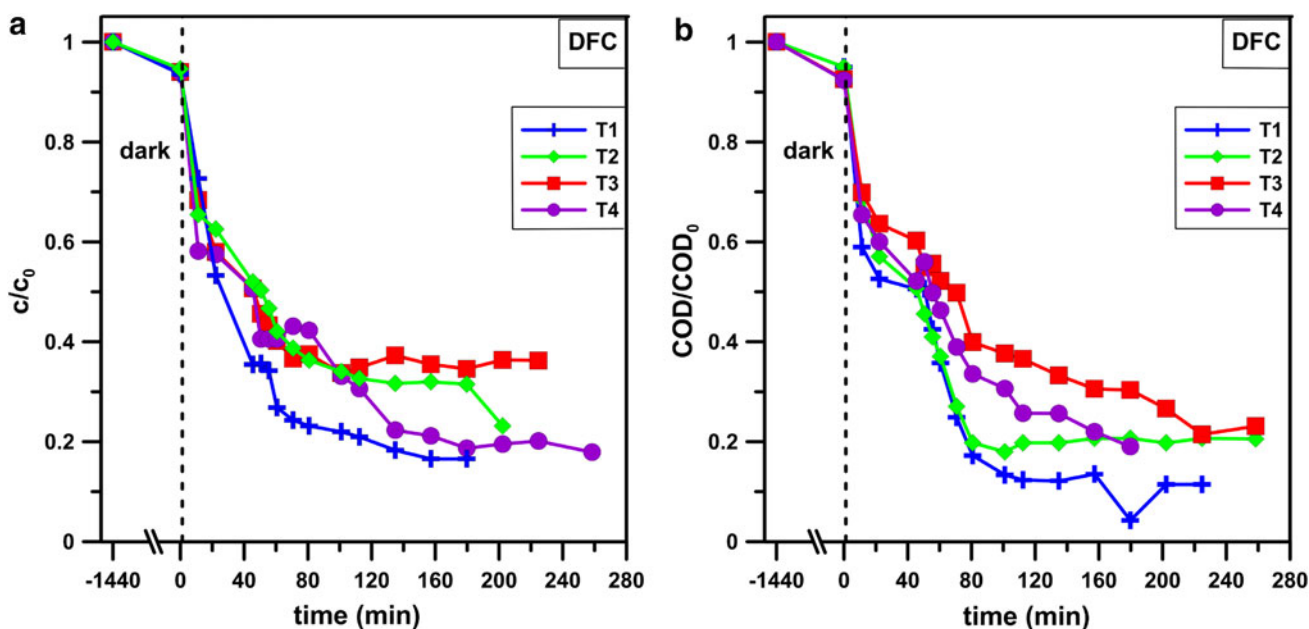


Fig. 5 The DFC photocatalytic removal from water a DFC concentration determined by UV-Vis spectrophotometer, b COD of treated wastewater containing DFC (Color figure online)

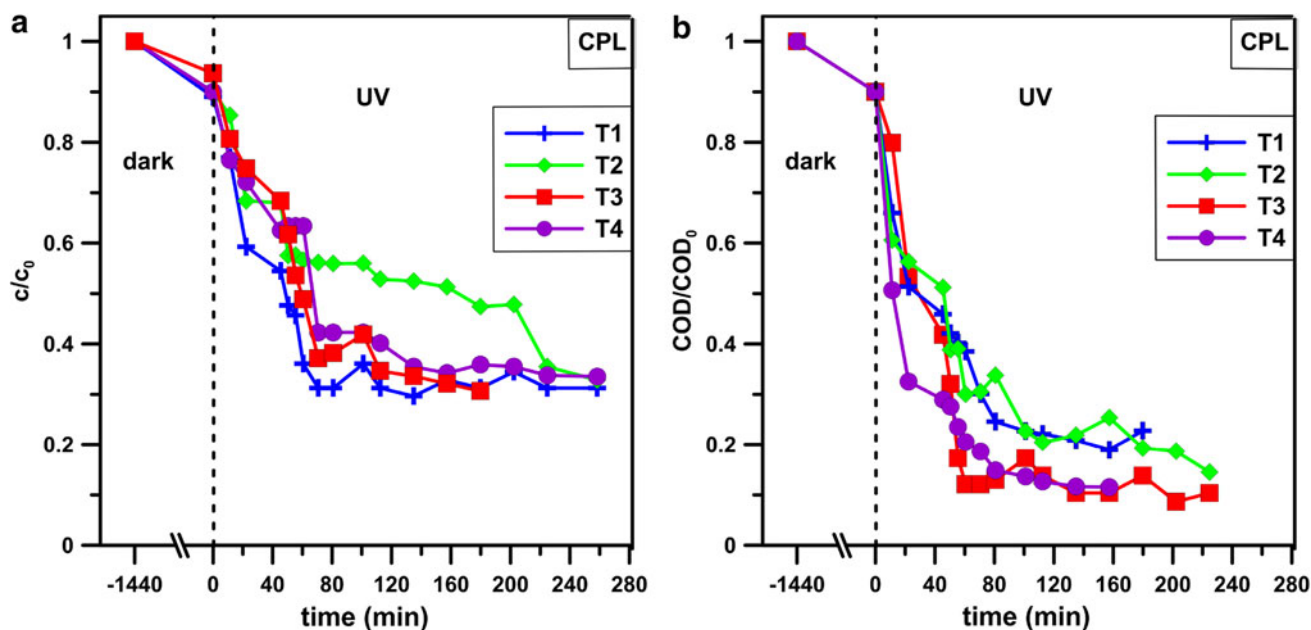


Fig. 6 The photocatalytic removal of **a** CPL and **b** COD of treated water containing CPL (Color figure online)

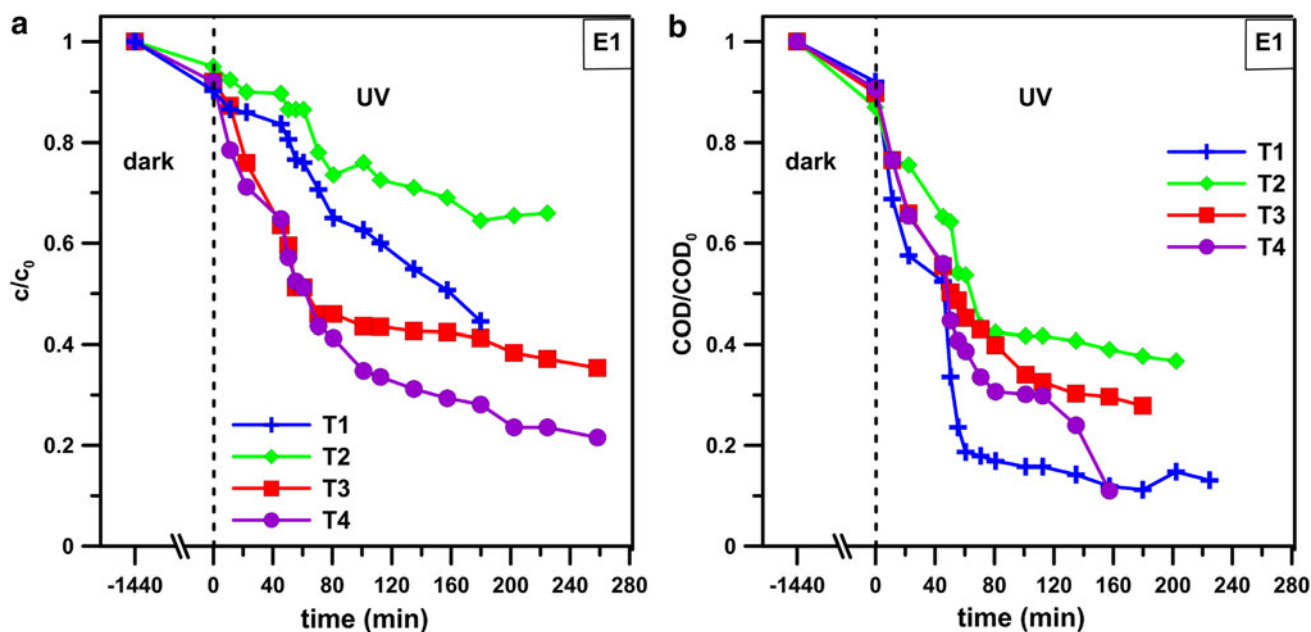


Fig. 7 The photocatalytic removal of **a** E1 and **b** COD of treated water containing E1 (Color figure online)

pollutant possessed electroneutral characteristics. The pH value of finally treated wastewater dropped to 7. It was observed by Liu and Liu 2004, that $\text{pH} = 7$ was the most suitable for the photolysis of E1. The mechanism of photooxidation is described as the breakage and oxidation of benzene rings to produce compounds containing carbonyl groups.

3.2.4 Mt photoremoval

The presented in Fig 8 photocatalytic oxidation of Mt proceeded the most effectively using T3. This photocatalyst was the most suitable both for Mt photoremoval and COD reduction of water containing Mt. The lowest activity was obtained for T2. The presence of rutile and the highest

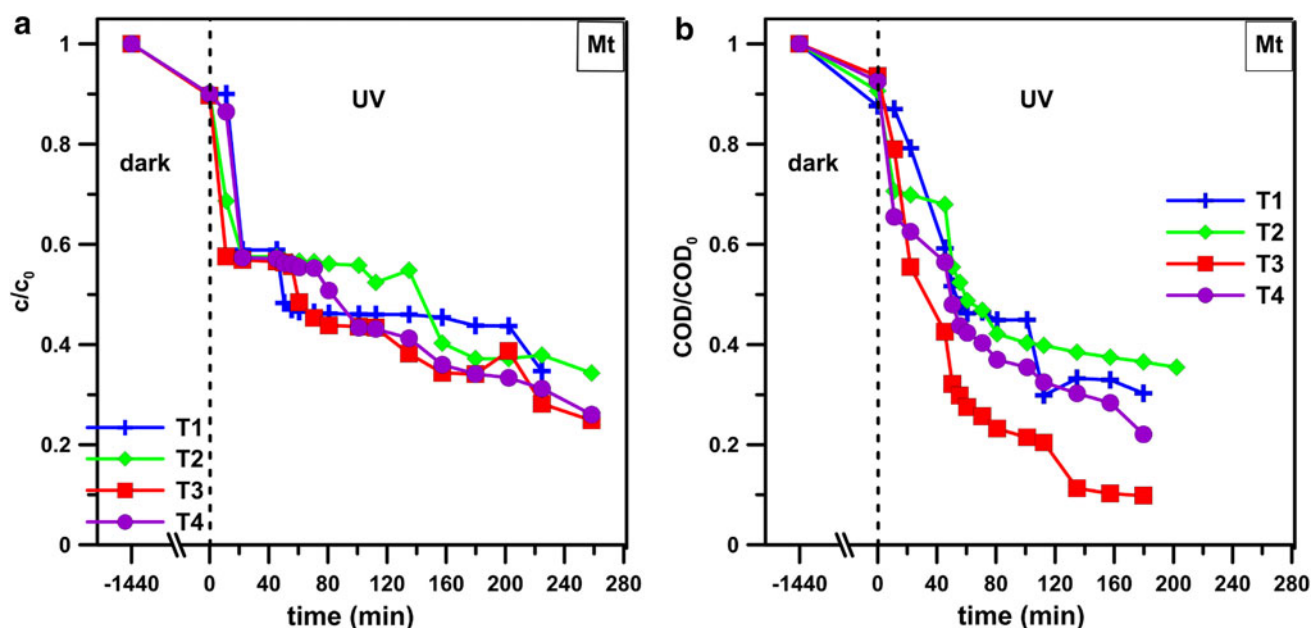


Fig. 8 The photocatalytic removal of **a** Mt and **b** COD of treated water containing Mt (Color figure online)

surface area favored the Mt photooxidation. The curves describing the Mt removal using both anatases proceeded similarly. The photocatalysts with lowest S_{BET} value revealed the lowest activity in Mt photocatalytic oxidation. The results of COD reduction indicated that the process proceeded with almost the same activity for all studied photocatalysts but during initial 60 min of treatment, still, T2 did not enhanced the photoremoval.

The pH of the water with Mt was 6.888 indicated that adsorption occurred via electrostatic forces. Final pH of treated water was 7.5.

3.3 Kinetics of photooxidation

For the determination of the kinetic data of Dc photooxidation a preliminary power law kinetic model was applied (Eq. 4) (Herrmann 2010):

$$r = -\frac{dc}{dt} = kc^n \tag{4}$$

where r , c and t represent the rate of degradation, pollutants concentration and time respectively. Also k and n are the rate constant and reaction order.

From the dark phase measurements of different TiO_2 photocatalysts (Martinez et al. 2011), the photocatalytic degradation of DFC using UV–Vis can be adequately described using a modified Langmuir–Hinshelwood kinetic model that when the surface of the catalyst is homogeneous, can be simplified to the first order kinetic model (Eq. 5):

$$r = k_{app} \cdot c \tag{5}$$

where k_{app} would be the apparent pseudo-first order kinetic rate constant. The initial concentration of the organic substrate c_0 was kept constant to simplify the heterogeneous photocatalytic process.

The rate constants per unit reactor volume k_l , which includes the effect of radiation absorption, were obtained by fitting the experimental data from the relation (Eq. 6):

$$-\ln(c/c_0) = k_l t \tag{6}$$

where c_0 and c are initial and determined at time t (min) concentration, k_l is the pseudo first-order rate constant (min^{-1}). The k_l was determined from the slope of the linear regressions obtained by plotting $-\ln(c/c_0)$ versus time. Since all experiments were carried at equal level of photon absorption this effect was the same for all photocatalysts. The apparent rate constants of the catalyst per mass unit (k_w) and per surface area unit (k_s) were estimated from Eqs. 7 and 8 (Dolat et al. 2012):

$$k_w = \frac{k_l}{c_w \cdot V_r} \tag{7}$$

$$k_s = \frac{k_l}{S_{BET} \cdot c_w \cdot V_r} \tag{8}$$

where c_w was the concentration of the photocatalysts, S_{BET} BET surface of photocatalyst and V_r —reactor volume (0.3 dm^3). Consequently, half-lives were calculated using Eq. 9:

$$t_{1/2} = \frac{0.6931}{k_1} \tag{9}$$

Table 3 The kinetic data obtained for the studied photocatalysts: apparent rate constants of DFC, CPL, Mt and E1 degradation per unit reactor volume (k_I), per gram of catalyst (k_w) and per unit surface area of catalyst (k_s) and initial reaction rate (r_0)

Catalyst	Kinetic parameter		Compound			
			DCF	E1	CFL	Mt
T1	k_I	($\times 10^{-2}$) (min^{-1})	1.3476	0.4518	1.2007	0.5758
	k_w	($\times 10^{-2}$) ($\text{min}^{-1} \text{g}^{-1}$)	0.308	0.103	0.276	0.131
	k_s	($\times 10^{-4}$) ($\text{min}^{-1} \text{m}^{-2}$)	2.547	0.854	2.283	1.088
	$t_{1/2}$	(min)	51.43	153.41	57.38	120.37
	R^2	–	0.93	0.99	0.99	0.95
	r_0	($\times 10^{-6}$) ($\text{mol}\cdot\text{dm}^{-2} \text{min}^{-1}$)	1.324	1.869	0.836	1.077
T2	k_I	($\times 10^{-2}$) (min^{-1})	0.8591	0.2353	0.8497	0.4771
	k_w	($\times 10^{-2}$) ($\text{min}^{-1} \text{g}^{-1}$)	0.196	0.054	0.194	0.109
	k_s	($\times 10^{-4}$) ($\text{min}^{-1} \text{m}^{-2}$)	0.321	0.088	0.318	0.947
	$t_{1/2}$	(min)	80.68	294.56	81.57	145.27
	R^2	–	0.95	0.99	0.95	0.92
	r_0	($\times 10^{-6}$) ($\text{mol dm}^{-2} \text{min}^{-1}$)	1.350	1.215	0.435	0.892
T3	k_I	($\times 10^{-2}$) (min^{-1})	0.6982	0.5442	0.8840	0.3300
	k_w	($\times 10^{-2}$) ($\text{min}^{-1} \text{g}^{-1}$)	0.159	0.124	0.202	0.075
	k_s	($\times 10^{-4}$) ($\text{min}^{-1} \text{m}^{-2}$)	0.261	0.204	1.755	0.028
	$t_{1/2}$	(min)	99.27	127.36	78.41	210.03
	R^2	–	0.90	0.90	0.95	0.92
	r_0	($\times 10^{-6}$) ($\text{mol dm}^{-2} \text{min}^{-1}$)	1.097	1.368	1.006	0.617
T4	k_I	($\times 10^{-2}$) (min^{-1})	0.8782	0.7456	0.5162	0.6134
	k_w	($\times 10^{-2}$) ($\text{min}^{-1} \text{g}^{-1}$)	0.201	0.170	0.118	0.141
	k_s	($\times 10^{-4}$) ($\text{min}^{-1} \text{m}^{-2}$)	0.362	0.308	0.213	0.058
	$t_{1/2}$	(min)	78.92	92.96	134.27	112.99
	R^2	–	0.97	0.95	0.92	0.94
	r_0	($\times 10^{-6}$) ($\text{mol dm}^{-2} \text{min}^{-1}$)	1.8025	0.7987	1.3789	1.1471

According to the obtained results it can be deduced that the degradation of studied pollutants may be generally described by pseudo-first order kinetics (Table 3). That is with agreement with data obtained by Zhang et al. (2011) for DFC, Liu and Liu (2004) for E1.

The closer analysis revealed, however, that two steps during the process may be observed. The identification of the process during first 45 min of treatment needs further studies.

The determined k_I values are changing in the following order:

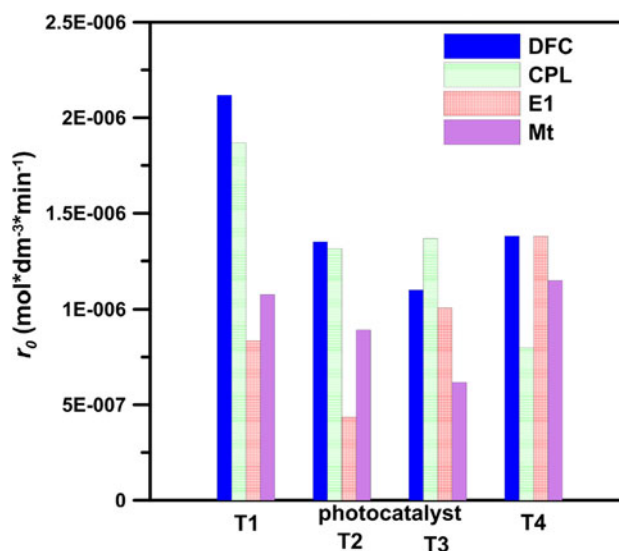
DCF T1 > T4 > T2 > T3 with the difference between the lowest and the highest value about 100 %

E1 T4 > T3 > T1 > T2 with almost three times higher k_I value for T4 than T1

CPL T1 > T3 > T2 > T4 with k_I determined for T4 was two times higher than k_I for T2

Mt T4 > T1 > T2 > T3 with the similar value obtained for anatase TiO_2

The presence of rutile has not always the detrimental effect on the removal of studied pollutants. For DFC and Mt

**Fig. 9** The relation of initial reaction rate with the type of the photocatalysts (Color figure online)

removal the anatase structure favored the photocatalytic oxidation. The intermediate effect was observed for CPL and E1. The key however was not only the presence of rutile but rather surface properties of studied photocatalysts.

Taking into consideration that the process of heterogeneous photocatalysis depends on the total surface area and affordability of active centers on the photocatalyst surface, the relation of initial reaction rate (r_0) versus S_{BET} was presented in Fig. 9.

It can be observed that over T4 almost all pollutants were removed with similar initial reaction rate. It is worth noting that generally the initial reaction rate of the removal of DFC and CPL did not differ significantly. However, the linear dependency of r_0 with the S_{BET} was not observed for any of the photocatalysts.

4 Conclusions

According to the obtained results it may be concluded:

- The time dependence of treatment of studied pollutants revealed that the best changes in the water condition were observed during first hour of treatment and further prolongation of treatment time till 4 h. did not result in the total removal of pollutants because produced by- and end-products of photooxidation were stable and resistant to further oxidation what may suggest that, the photocatalytic treatment using described photocatalysts and reactor configuration can not totally solve the environmental hazards arising from PPCPs;
- The presence of rutile and large TiO_2 crystals in TiO_2 slightly diminished the photocatalytic efficiency of DFC removal;
- The mineralization of DFC over T3 was as fast as the DFC photoremoval;
- The photooxidation of CPL proceeded faster over smaller crystals of TiO_2 and the photocatalysts with enhanced surface area were more effective than their low surface area counterparts;
- The similar general tendency for low and high surface area photocatalysts can be observed during E1 removal;
- The presence of rutile and the highest surface area favored the Mt photooxidation. The photocatalysts with lowest S_{BET} value revealed the lowest activity in Mt photocatalytic oxidation.
- The photooxidation of all studied pollutants followed the pseudo-first order kinetics.

Acknowledgments Grupa Azoty (formerly Zakłady Azotowe Police) is truly acknowledged for the samples of Tytanpol TiO_2 . The authors also appreciate the anonymous reviewers whose excellent comments improved significantly the quality of this manuscript.

Open Access This article is distributed under the terms of the Creative Commons Attribution License which permits any use, distribution, and reproduction in any medium, provided the original author(s) and the source are credited.

References

- Achilleos, A., Hapeshi, E., Xekoukoulotakis, N.P., Mantzavinos, D., Fatta-Kassinos, D.: Factors affecting diclofenac decomposition in water by UV-A/ TiO_2 photocatalysis. *Chem. Eng. J.* **161**, 53–59 (2010)
- Álvarez, P.M., Jaramillo, J., López-Piñero, F., Plucinski, P.K.: Preparation and characterization of magnetic TiO_2 nanoparticles and their utilization for the degradation of emerging pollutants in water. *Appl. Catal. B: Environ.* **100**, 338–345 (2011)
- Chong, M.N., Jin, B., Chow, Ch.W.K., Saint, Ch.: Recent developments in photocatalytic water treatment technology: a review. *Water Res.* **44**, 2997–3027 (2010)
- Dolat, N., Quici, E., Kusiak-Nejman, A.W., Morawski, G., Li Puma: One-step, hydrothermal synthesis of nitrogen, carbon co-doped titanium dioxide (N,C TiO_2) photocatalysts. Effect of alcohol degree and chain length as carbon dopant precursors on photocatalytic activity and catalyst deactivation. *Appl. Catal. B: Environ.* **115–116**, 81–89 (2012)
- Ellis, J.B.: Pharmaceutical and personal care products (PPCPs) in urban receiving waters. *Environ. Poll.* **144**, 184–189 (2006)
- Emeline, A.V., Zhang, X., Murakami, T., Fujishima, A.: Activity and selectivity of photocatalysts in photodegradation of phenols. *J. Hazard. Mat.* **211–212**, 154–160 (2012)
- Fatta-Kassinos, D., Vasquez, M.I., Kümmerer, K.: Transformation products of pharmaceuticals in surface waters and wastewater formed during photolysis and advanced oxidation processes—degradation, elucidation of byproducts and assessment of their biological potency. *Chemosphere* **85**, 693–709 (2011)
- Fernandez, A., Lassaletta, G., Jimenez, V.M., Justo, A., Gonzalez-Elipse, A.R., Herrmann, J.-M., Tahiri, H., Ait-Ichou, Y.: Preparation and characterization of TiO_2 photocatalysts supported on various rigid supports (glass, quartz and stainless steel). Comparative studies of photocatalytic activity in water purification. *Appl. Catal. B.* **7**, 49–63 (1995)
- Friedmann, D., Mendive, C., Bahnemann, D.: TiO_2 for water treatment: parameters affecting the kinetics and mechanisms, of photocatalysis. *Appl. Catal. B.* **99**, 398–406 (2010)
- Gultekin, I., Ince, N.H.: Synthetic endocrine disruptors in the environment and water remediation by advanced oxidation processes Review. *J. Environ. Mgmt* **85**, 816–832 (2007)
- Hapeshi, E., Achilleos, A., Vasquez, M.I., Michael, C., Xekoukoulotakis, N.P., Mantzavinos, D., Kassinos, D.: Drugs degrading photocatalytically: kinetics and mechanisms of ofloxacin and atenolol removal on titania suspensions. *Water Res.* **44**, 1737–1746 (2010)
- He, Z., Zhu, Z., Li, J., Zhou, J., Wei, N.: Characterisation and activity of mesoporous titanium dioxide beads with high surface areas and controllable pore sizes. *J. Hazard. Mat.* **190**, 133–139 (2011)
- Herrmann, J.-M.: Photocatalysis fundamentals revisited to avoid several misconceptions. *Appl. Catal. B.* **99**, 461–468 (2010)
- Ioannou, L.A., Hapeshi, E., Vasquez, M. I., Mantzavinos, D., Fatta-Kassinos, D.: Solar/ TiO_2 photocatalytic decomposition of β -blockers atenolol and propranolol in water and wastewater. *Sol. Energy* **85**, 1915–1926 (2011)
- Jelic, A., Gros, M., Ginebreda, A., Cespedes-Sánchez, R., Ventura, F., Petrovic, M., Barcelo, D.: Occurrence, partition and removal of pharmaceuticals in sewage water and sludge during wastewater treatment. *Water Res.* **45**, 1165–1176 (2010)

- Kasperek, R., Świąder, K., Zuń, M., Belniak, P., Zimmer, Ł., Dobiecka, E., Poleszak, E.: Influence of the type of the dissolution medium on the UV spectra of diclofenac sodium. *ANNALES Universitatis Mariae Curie-Skłodowska Lublin-Polonia, SECTIO DDD XXIV*, 39–45 (2011)
- Kasprzyk-Hordern, B., Dinsdale, R.M., Guwy, A.J.: The removal of pharmaceuticals, personal care products, endocrine disruptors and illicit drugs during wastewater treatment and its impact on the quality of receiving waters. *Water Res.* **43**, 363–380 (2009)
- Kim, I., Yamashita, N., Tanaka, H.: Photodegradation of pharmaceuticals and personal care products during UV and UV/H₂O₂ treatments. *Chemosphere* **77**, 518–525 (2009)
- Kumar, S., Ravikumar, R., Rajasekaran, A., Ravichandran V.: Simultaneous spectrophotometric determination of metoprolol tartrate and ramipril. *Digest J. Nanomater. Biostruct* **5**, 173–176 (2010)
- Liu, B., Liu, X.: Direct photolysis of estrogens in aqueous solutions. *Sci. Total Environ.* **320**, 269–274 (2004)
- Lopez, A., Bozzi, A., Mascolo, G., Kiwi, J.: Kinetic investigation on UV and UV/H₂O₂ degradations of pharmaceutical intermediates in aqueous solution. *J. Photochem. Photobiol. A* **156**, 121–126 (2003)
- Martínez, C., Canle, M.L., Fernández, M.I., Santaballa, J.A., Faria, J.: Aqueous degradation of diclofenac by heterogeneous photocatalysis using nanostructured materials. *Appl. Catal. B: Environ.* **107**, 110–118 (2011)
- Qin, M., Yang, H., Chen, S., Xie, H., Guan, J.: Photochemical characteristics of diclofenac and its photodegradation of inclusion complexes with β -cyclodextrins. *Quim. Nova* **35**, 559–562 (2012)
- Sanderson, H., Johnson, D.J., Reitsma, T., Brain, R.A., Wilson, C.J., Solomon, K.R.: Ranking and prioritization of environmental risks of pharmaceuticals in surface waters. *Regul. Toxicol. Pharmacol.* **39**, 158–183 (2004)
- Ternes, T.A., Stuber, J., Herrmann, N., McDowell, D., Ried, A., Kampmann, M., Teiser, B.: Ozonation: a tool for removal of pharmaceuticals, contrast media and musk fragrances from wastewater? *Water Res.* **37**, 1976–1982 (2003)
- Yao, S., Li, J., Shi, Z.: Immobilization of TiO₂ nanoparticles on activated carbon fiber and its photodegradation performance for organic pollutants. *Particuology* **8**, 272–278 (2010)
- Zhang, N., Liu, G., Liu, H., Wang, Y., He, Z., Wang, G.: Diclofenac photodegradation under simulated sunlight: effect of different forms of nitrogen and Kinetics. *J. Hazard. Mat.* **192**, 411–418 (2011)